Journal of Hydrology 468–469 (2012) 151–158

Contents lists available at SciVerse ScienceDirect

Journal of Hydrology

journal homepage: www.elsevier.com/locate/jhydrol

Response of epikarst hydrochemical changes to soil CO_2 and weather conditions at Chenqi, Puding, SW China

Rui Yang, Zaihua Liu *, Cheng Zeng, Min Zhao

State Key Laboratory of Environmental Geochemistry, Institute of Geochemistry, Chinese Academy of Sciences, 46 Guanshui Road, Guiyang 550002, China
Puding Comprehensive Karst Research and Experimental Station, Institute of Geochemistry, CAS and Science and Technology Department of Guizhou Province, Puding 562100, China

ARTICLE INFO

Article history:
Received 31 March 2012
Received in revised form 25 July 2012
Accepted 16 August 2012
Available online 25 August 2012
This manuscript was handled by Laurent Charlet, Editor-in-Chief, with the assistance of Nico Goldscheider, Associate Editor

Keywords:
Epikarst spring
Hydrochemical variations
Soil CO_2 effect
Dilution effect
High-resolution monitoring strategy
Global carbon cycle

SUMMARY

Karst processes-related carbon cycle, as a result of the water–carbonate rock–CO_2 gas–aquatic organism interaction, significantly affects global carbon budget. In karst areas, soil CO_2 is a major chemical driving force for the karst processes and has significant impact on the geochemical processes of the water–rock–gas–organism system. Currently, there have been many studies mainly focusing on the hydrochemical responses of the epikarst water system to weather conditions. However, few studies examine the direct correlation between the hydrochemical parameters in epikarst systems and soil CO_2. We chose an epikarst spring system at Chenqi, Puding, SW China to monitor both the concentration of soil CO_2 and hydrochemical parameters at high-resolution (every 15 min) during July 2010–December 2011 covering a complete hydrologic year, and to investigate the response of hydrochemical changes to soil CO_2 and weather conditions. It was found that both soil CO_2 and rainfall are the major driving forces for the epikarst hydrochemical variations. The soil CO_2 effect on hydrochemical variations was reflected in all seasonal, diurnal and storm-scales. There was an increase in pCO_2 and electrical conductivity (EC) but a decrease in pH caused by the increase in soil CO_2 in spring-summer growing season, while a decrease in pCO_2 and EC but an increase in pH caused by the decrease in soil CO_2 happened in autumn–winter dormant season. Similar variations were also found on diurnal scales but with a time lag of a few hours between hydrochemical changes and soil CO_2 change during dry season, showing effect of the groundwater recharge mode as well as the complexity of the supply path (quick flow by conduit or slow flow by fracture). During rainy seasons, however, hydrochemical changes in epikarst groundwater were regulated by both dilution and soil CO_2 effects. Under high-intensity rainfall, the dilution effect was dominant, indicated by a quick decrease in EC, pH and calcite saturation (SIc) but a quick increase in pCO_2. In contrast, under low-intensity rainfall, the soil CO_2 effect was dominant, indicated by an increase in EC and pCO_2 but a decrease in pH and SIc. To sum up, this study has shown the high sensitivity and variability of epikarst processes to the environmental change, implying that the role of karst processes in the global carbon cycle needs to be reappraised based on high-resolution monitoring strategy.

1. Introduction

The increased concentration of greenhouse gases in the atmosphere could change the energy equilibration and thus affect the global climate (Manabe and Stouffer, 1979). In company with increasing world population and the development of human society, continuous global warming due to the increase of greenhouse gases, especially CO_2, becomes serious. To alleviate this problem, global carbon cycle including source and sink has attracted great attention (Jenkinson et al., 1991; Lasco et al., 2002; Liu et al., 2010).

Karst processes-related carbon cycle, as a result of the water–carbonate rock–CO_2 gas–aquatic organism interaction, significantly affects global carbon budget (Yuan, 1997; Liu et al., 2010, 2011). A series of hydrogeochemical processes accompanied by the water–rock–gas–organism interaction will lead to the hydrochemical variations of groundwater (Liu et al., 2004, 2006, 2007), from which we could infer the driving forces for the variations. It is generally known that soil CO_2 is a major chemical driving force for carbonate dissolution and has a significant influence on groundwater hydrochemical features (Morse and Arvidson, 2002; Ford and Willams, 2007; Liu et al., 2007; Zhao et al., 2010). Fig. 1 shows the major processes of the generation, migration and conversion of soil CO_2. Soil CO_2 formed by root respiration and microbial decomposition diffuses to the atmosphere as an upward flux called soil respiration while part of it dissolves in soil water as corrosive H_2CO_3 which could further react with carbonates and finally

* Corresponding author at: State Key Laboratory of Environmental Geochemistry, Institute of Geochemistry, Chinese Academy of Sciences, 46 Guanshui Road, Guiyang 550002, China. Fax: +86 851 5895263.
E-mail address: liuzaihua@vip.gyig.ac.cn (Z. Liu).

0022-1694/$ - see front matter © 2012 Elsevier B.V. All rights reserved.
http://dx.doi.org/10.1016/j.jhydrol.2012.08.029

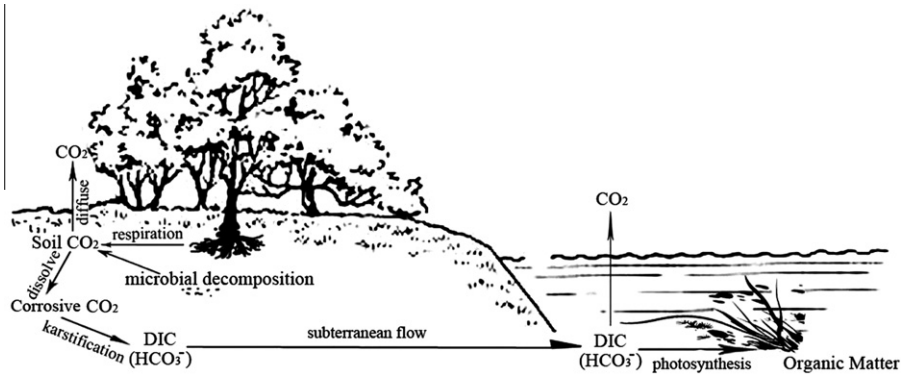

Fig. 1. The major processes of the generation, migration and conversion of soil CO_2, drawing in reference to Liu et al. (2010).

infiltrates into the groundwater (Brook et al., 1983; Jassal et al., 2004; Liu et al., 2007). HCO_3^- as one of the reaction products could be utilized by the photosynthesis of aquatic organisms and fixed as organic matter as a carbon sink when the groundwater is exposed to surface (Liu et al., 2010; Sun et al., 2011).

However, CO_2-driving force of hydrochemical variations, lacking high-resolution data support, is mainly based on theoretical inferences. On the basis of field survey, an epikarst spring system at Chenqi, Puding, SW China was chosen to monitor both the concentration of soil CO_2 and hydrochemical parameters at high-resolution (every 15 min) during July 2010–December 2011 covering a complete hydrologic year, and to investigate the response of hydrochemical changes to soil CO_2 and weather conditions. It was found that both soil CO_2 and rainfall are the major driving forces for the hydrochemical variations in the epikarst system. The soil CO_2 effect on hydrochemical variations was reflected in all seasonal, diurnal and storm-scales, showing the high sensitivity and variability of epikarst processes to eco-environmental change, and thus the role of karst processes in the global carbon cycle needs to be reappraised based on high-resolution monitoring strategy.

Fig. 2. The plot for sampling soil with rich vegetation cover in the summer growing season (photo taken on September 9, 2011).

2. Site description

The Chenqi epikarst karst system is located in Puding County, Guizhou Province, China. The climatic condition here is characterized by humid subtropical monsoon climate with annual mean precipitation of 1315 mm (over 80% of precipitation occurs during the rainy season from May to October) and mean air temperature of about 15.1 °C. The main lithology is limestone and dolomite of the Guanling Formation of middle Triassic, intercalated with gypsum strata (Zhao et al., 2010).

The main geomorphology of Chenqi is a typical karst valley. As plot for sampling soil and ground water (Fig. 2), we chose an abandoned arable land at the mountainside with an altitude about 1350 m and an epikarst spring named Wantian by the foot of the mountain (Fig. 3). The relative elevation between them is about 20 m.

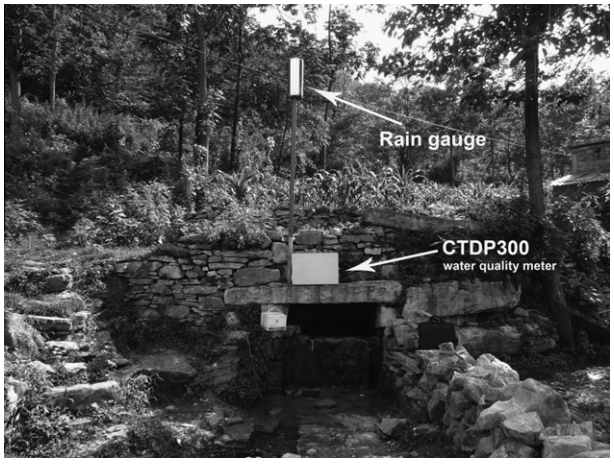

Fig. 3. Wantian epikarst spring (photo taken on July 14, 2010).

3. Methods

3.1. Automatic data logging

To obtain soil CO_2 concentration, soil temperature and humidity data, a composite measurement system, including GMM221 (CO_2 sensor made by VAISALA in Finland with the measuring range from 0% to 10% and resolution of 1 ppm), AV-EC5 and AV-10T (humidity and temperature sensors produced by AVALON in America with a resolution of 0.1% and 0.1 °C respectively), was set up at the sample soil plot (Fig. 2). All the sensors were imbedded into soil at the depth of 60 cm by drilling. A CTDP300 multi-parameter water quality meter (made by Greenspan Corporation in Australia) was placed at the spring (Fig. 3) to obtain detailed hydrochemical variations by logging rainfall, water stage, water temperature, pH and electrical conductivity (EC), with a resolution of 0.5 mm, 0.1 cm,

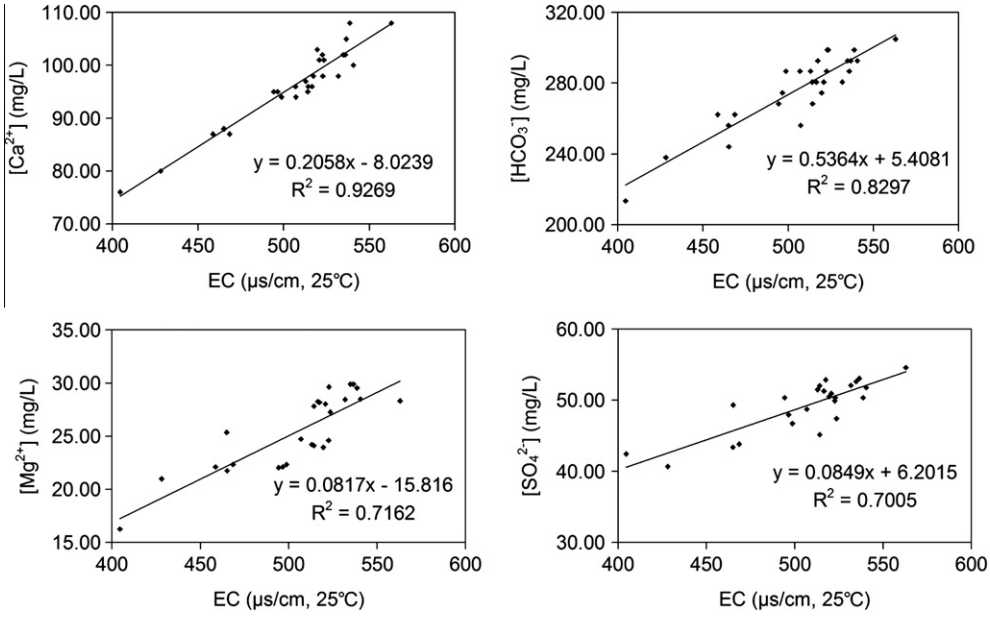

Fig. 4. Linear relationships between specific conductivity versus $[Ca^{2+}]$, $[Mg^{2+}]$, $[HCO_3^-]$ and $[SO_4^{2-}]$, respectively, for the Wantian epikarst spring.

0.01 °C, 0.01 pH and 0.01 μS/cm respectively (Liu et al., 2007). Both the CO_2 measurement system and the water quality data logger were set to monitor the synchronous changes at a same time-interval of 15 min.

The sensors and probes were calibrated prior to deployment. We used a CO_2 portable analyzer (GM70, made in Finland) and hand-held water quality meter (WTW350i, made in Germany) monthly to check the reliability of automatic measurements. Hydrochemical data measured by WTW350i and CTDP300 was identical with one standard error <2%. However, CO_2 concentration measured by GM70 was always lower than the automatic records with one standard error of about 10% (Fig. 5). The main reason may be that, compared with the closed environment for GMM221 measurement (CO_2 sensor was buried underground, and thus closed to open air), the depth where GM70 probe located at was not tight enough, and thus diffuse of soil CO_2 to atmosphere was getting faster, leaving the lower soil CO_2 value. In addition, the amount of rainfall recorded by CTDP300 was compared with the rainfall records from the nearest meteorological station (about 600 m apart), which showed little difference (~1%).

3.2. In situ titration and major ions analysis

$[HCO_3^-]$ and $[Ca^{2+}]$ were measured in the field using the Aquamerck alkalinity test kit and the hardness test kit monthly (Zolotov et al., 2002; Banks and Frengstad, 2006; Liu et al., 2007), with an estimated accuracy of 0.05 mmol/L and 1 mg/L respectively.

Two sets of water samples were filtered through 0.45 μm Millipore filters into 60 mL acid-washed high-density polyethylene bottles for conventional ion analysis. The cations test samples were acidified to pH < 2.0 by using concentrated nitric acid to prevent complexation and precipitation. The samples were taken back to the laboratory to determine cations concentrations of Na^+, K^+, Ca^{2+}, and Mg^{2+} through the use of the inductively coupled plasma optical emission spectrometer (ICP-OES) and anions concentrations of SO_4^{2-}, Cl^-, and NO_3^- by ion chromatography (Banks and Frengstad, 2006; Zhao et al., 2010).

3.3. Hydrochemical model calculation

CO_2 partial pressure (pCO_2) and calcite saturation index (SIc) are important hydrochemical parameters in karst research. They could be calculated from a geochemical model with pH, temperature and seven major ions concentrations (Liu et al., 2007; Zhao et al., 2010). As mentioned before, the main lithology in this region is limestone and dolomite, intercalated with gypsum strata. Thus, Ca^{2+} and Mg^{2+} are the major cations while HCO_3^- and SO_4^{2-} are the major counterbalancing anions in the spring because of the dissolution of calcite, dolomite and gypsum. These preponderating ions dominate the electrical conductivity (EC) in the water. Consequently, continuous concentrations of Ca^{2+}, Mg^{2+}, HCO_3^- and SO_4^{2-} were estimated through the automatically recorded data of EC. From the monthly data of in situ titration and samples analysis,

Table 1
Minimum, maximum and annual mean values of soil temperature (soil temp.), soil CO_2, water temperature (water temp.), electrical conductivity (EC) and hydrochemical parameters in Wantian Spring.

Item	Soil temp. (°C)	Soil CO_2 (Pa)	Water temp. (°C)	pH	K^+ (mg/L)	Na^+ (mg/L)	Ca^{2+} (mg/L)	Mg^{2+} (mg/L)	Cl^- (mg/L)	SO_4^{2-} (mg/L)	HCO_3^- (mg/L)	NO_3^- (mg/L)	EC (μS/cm 25 °C)	SIc[a]	pCO_2[b] (Pa)
Min.	3.18	302.2	12.54	6.91	0.40	0.05	76.00	14.55	0.80	32.53	201.30	0.29	383.25	−0.43	237.7
Max.	26.60	2852.4	20.25	7.95	2.35	1.35	146.00	35.65	5.40	56.92	396.50	6.74	608.86	0.79	2142.7
Mean	15.73	1458.9	16.43	7.65	0.85	0.52	95.50	24.70	2.99	49.05	273.89	2.40	513.10	0.46	598.1
N	32,137	36,577	50,793	50,793	18	18	18	18	18	18	18	18	50,793	50,793	50,793

N means number of samples.

[a] Calcite saturation index in water (SIc = log IAP/*K*, where IAP is ionic activity product and *K* is the calcite equilibrium constant). If SIc > 0, supersaturation occurs and travertine may deposit; if SIc < 0, water is aggressive to calcite; and if SIc = 0, the equilibrium reaches.

[b] Calculated CO_2 partial pressure of water by WATSPEC (Wigley, 1977).

Table 2
Correlations between soil CO_2, pH and electrical conductivity (EC) and soil temperature (soil temp.).

	Soil temp.	Soil CO_2	pH	EC
Soil temp.				
Pearson correlation	1	.851**	−.635**	.508**
Sig. (2-tailed)		.000	.000	.000
N	32,137	32,137	32,137	32,137
Soil CO_2				
Pearson correlation	.851**	1	−.493**	.329**
Sig. (2-tailed)	.000		.000	.000
N	32,137	36,577	36,577	36,577
pH				
Pearson correlation	−.635**	−.493**	1	.115**
Sig. (2-tailed)	.000	.000		.000
N	32,137	36,577	50,793	50,793
EC				
Pearson correlation	.508**	.329**	.115**	1
Sig. (2-tailed)	.000	.000	.000	
N	32,137	36,577	50,793	50,793

N means number of samples.
** Correlation is significant at the 0.01 level (2-tailed).

the linear relationship between concentrations of these ions and EC was established (Fig. 4):

$$[Ca^{2+}] = 0.2058EC - 8.0239, \quad r^2 = 0.9269 \tag{1}$$

$$[Mg^{2+}] = 0.0817EC - 15.816, \quad r^2 = 0.7162 \tag{2}$$

$$[HCO_3^-] = 0.5364EC + 5.4081, \quad r^2 = 0.8297 \tag{3}$$

$$[SO_4^{2-}] = 0.0849EC + 6.2015, \quad r^2 = 0.7005 \tag{4}$$

where brackets denote species concentrations in mg/L and EC is specific conductivity in μS/cm at 25 °C.

It should be noted that EC is a linear relation of the concentrations of all ions in the solution. In fact, only for the clean limestone and dolomite waters (sulfates, nitrates and chlorides (SNC) < 10%, Krawczyk and Ford, 2006), the concentration of each species (Ca^{2+}, Mg^{2+}, HCO_3^-) is related to the other ones due to dissolution of these carbonate minerals. Although our case is not such a clean system (SNC ranging 17–20%, i.e., moderately contaminated according to Krawczyk and Ford (2006)), $[Ca^{2+}]$, $[Mg^{2+}]$, and $[HCO_3^-]$, which change synchronously, are the major variables in the system. Moreover, the empirical relations by plotting the measured concentrations versus EC seem nice (Fig. 4). So Eqs. (1)–(4) is a crude but acceptable approximation as others conducted before (Krawczyk and Ford, 2006; Zhao et al., 2010).

A program WATSPEC (Wigley, 1977), which calculates pCO_2 and SIc, was operated to process the full hydrochemical data sets, including recorded temperature and pH, concentrations of Ca^{2+}, Mg^{2+}, HCO_3^- and SO_4^{2-} calculated through the regression equations above, mean monthly values of K^+, Na^+, and Cl^-.

4. Results and discussion

Due to the extensive results of this work, summarizing the findings is difficult without reference to the full dataset. Since statistical analysis (Tables 1 and 2) does not convey the detail of the record, we present the data graphically in time series to allow visual assessment alongside the summary text. Three levels of time series are presented in Figs. 5–7 to show different details. Fig. 5 comprises the full data record, showing the seasonal variability with the fine detail of storm-scale fluctuations. Fig. 6a and b shows the more detailed diurnal fluctuations for a 2-day time series on August 30 to September 1 (growing season), 2010 and November 5–7 (dormant season), 2010 respectively. Storm-scale variations on September 6–11, 2010 are graphically represented in Fig. 7 to show how the rainfall and soil CO_2 affect the hydrochemical features of groundwater as well as the difference between dilution and soil CO_2 effects under different rainfall intensity.

The graphic results of the variations on these timescales we mentioned are analyzed as follows.

4.1. Variations of soil CO_2 concentration

The seasonal cycle of soil CO_2 concentration was remarkable (Fig. 5) though some data were missing due to the repairing of the sensor and/or logger. It shows in-phase change with soil temperature, i.e., increasing in spring and summer (from a few hundreds Pa to a few thousands Pa, with about an order of magnitude increase, Fig. 5) and decreasing in autumn and winter. In general, soil CO_2 originates mainly from root respiration and microbial decomposition (Hanson et al., 2000). In the spring-summer growing season, with the lush growth of plants (Fig. 2, implying higher root respiration) and the higher soil temperature (implying stronger microbial decomposition), soil CO_2 generation increases (Raich and Schlesinger, 1992; Atkin et al., 2000). This is the reason why soil CO_2 concentration was higher during summer than winter (Fig. 5) and may also explain the significant correlation between soil temperature and soil CO_2 ($R = 0.851$, Table 2).

The diurnal variations of soil CO_2, showing also in-phase change with soil temperature, are presented in Fig. 6a and b representing the spring-summer growing season and the autumn–winter dormant season respectively. In the spring-summer growing season, soil temperature and soil CO_2, rising to peaks at about 24:00 (Fig. 6a), are different from those in dormant autumn, reaching the maximum at about 14:00 (Fig. 6b). The most likely reason for this great time difference (10 h) is that, in the spring-summer growing season, the ground thermal response of the field site is mainly driven by solar radiation (Beltrami and Kellman, 2003), the plants in the sample soil plot (mainly weeds and dense secondary shrubs, see Fig. 2) flourish and cover the surface, blocking solar radiation and regulating the heat conduction between atmosphere and soil, thus delaying soil warming and the generation of soil CO_2 (Fig. 6a). In contrast, in the autumn–winter dormant season, most weeds wither to death and the soil could be heated directly by solar radiation with little vegetation cover (Cellier et al., 1996), therefore there is no or short time lag between soil temperature (soil CO_2) and air temperature (Fig. 6b).

During storm-scale time series, as shown in Fig. 7, soil CO_2 concentration declined rapidly after rainfall when much of soil CO_2 dissolved and migrated into the soil water and groundwater, which was evidenced by the abrupt increase in pCO_2 of the spring water after rainfall (Fig. 7).

4.2. Hydrochemical variations of the epikarst spring

4.2.1. CO_2 partial pressure and pH

Marked seasonal variations are found in Fig. 5 where CO_2 partial pressure (pCO_2) shows in-phase change with soil CO_2 (i.e., higher in summer and low in winter), while pH shows inverse change. The CO_2 partial pressure in water (pCO_2) directly affects pH fluctuation (Liu et al., 2006, 2007) and is strongly related to the soil CO_2. Due to the downward diffusion of soil CO_2, the more CO_2 in soil causes higher pCO_2 in water and thus lower pH. This was confirmed by statistical analysis with a R value of −0.493 between pH and soil CO_2 (Table 2).

The diurnal cycles of pH and pCO_2 are illustrated in the more detailed time series in Fig. 6a and b with a time lag of less than 1 h and about 6 h to the soil CO_2 change in growing season and dormant season respectively. It seems that the length of lag time

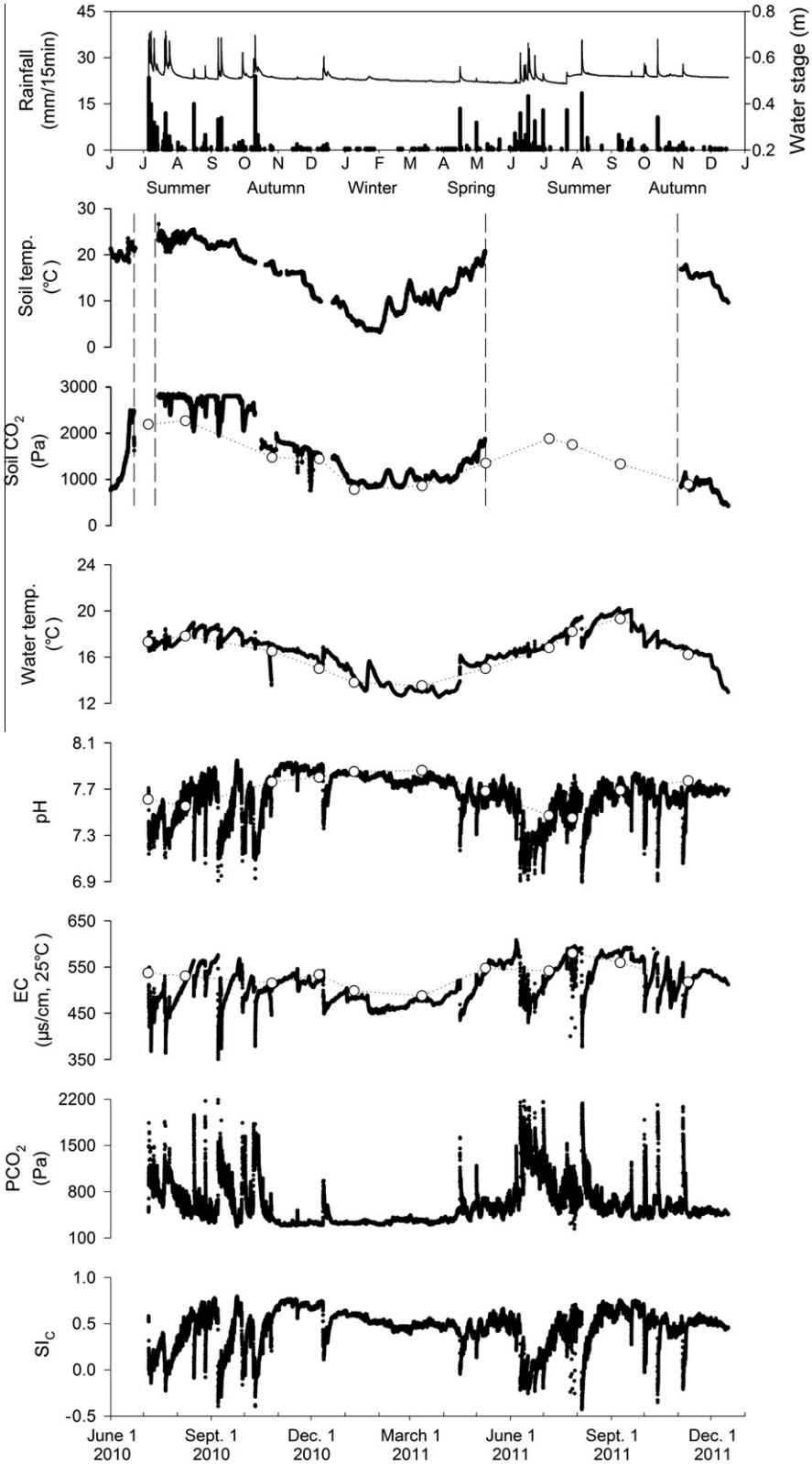

Fig. 5. Continuous data of soil temperature, soil CO_2 concentrations on the sample soil plot and hydrochemical parameters in Wantian Spring during July 2010–December 2011. The data between the two vertical dashed lines was not available due to repair of the sensor and/or logger. Open circles are those from the hand-held meters for checking.

depends on the groundwater recharge mode as well as the complexity of the supply path (quick flow by conduit or slow flow by fracture) (Atkinson, 1977; Denić-Jukić and Jukić, 2003; Birk et al., 2004). In the spring-summer rainy season, with abundant rainfall, soil moisture was higher and thus the dissolved CO_2 migrated into groundwater mainly through quick flow with a short lag time between pCO_2 (pH) and soil CO_2 (Fig. 6a). The situation in autumn–winter dry season was opposite and there was a longer lag time generally up to several hours because of the lower soil moisture and the slow flow in fracture (Fig. 6b).

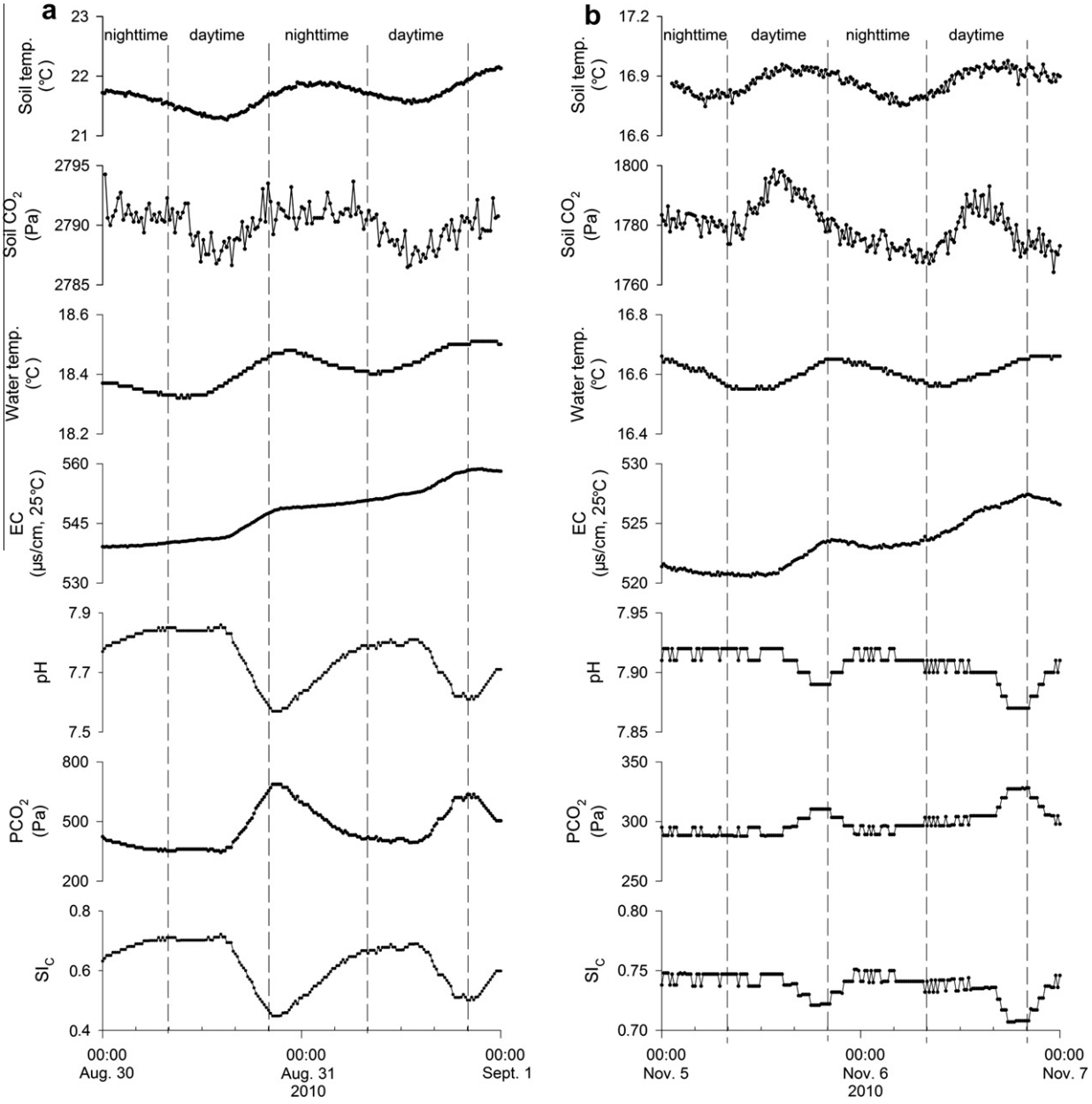

Fig. 6. (a) A 2-day diurnal variations in soil CO_2 concentrations on the sample soil plot and hydrochemical parameters in Wantian Spring at 15-min intervals, 30 August–1 September, 2010, where hydrochemical parameters and soil CO_2 show almost synchronous change with the time lag of less than 1 h. (b) A 2-day diurnal variations in soil CO_2 concentrations on the sample soil plot and hydrochemical parameters in Wantian Spring at 15-min intervals, 5–7 November, 2010, where hydrochemical parameters and soil CO_2 show asynchronous change with a time lag of about 6 h. Soil temperatures here were replaced by the data during the same time in 2011 because of the missing of data when repairing the sensor (the diurnal change of soil temperature should be similar though the absolute value could be different).

Storm-scale variations are also noticeable and presented in Fig. 7. Accompanied by the decline of soil CO_2 during rainfall, pCO_2 in water always increased while pH decreased as a result of the dissolution and infiltration of soil CO_2 through the soil/water system into the groundwater.

4.2.2. Electrical conductivity

Electrical conductivity (EC) varied noticeably (>50%) and showed in-phase change with soil CO_2 concentration on seasonal time scale (Fig. 5) and diurnal cycle (with a time lag of about 1 h and 6 h (Fig. 6a and b) in the summer rainy season and the autumn dry season respectively, like pCO_2 and pH as discussed above). EC depends on the level of ion concentrations in the water. In an epikarst water system, the ions originate mainly from the dissolution of calcite and dolomite in the CO_2–water solution (Liu et al., 2007). Therefore, when the soil CO_2 concentration is increasing, more corrosive CO_2–water solution is generated and causes stronger erosion and thus higher EC.

During rainy times, the variations of EC are indicative of different driving forces under different rainfall intensity (Fig. 7). Under heavy rainfall (t_1 and t_3 in Fig. 7), pCO_2 increased and pH decreased because of the dissolution and infiltration of soil CO_2 while EC declined due to the dominance of dilution effect of storm water over soil CO_2 effect (Liu et al., 2007). In contrast, under low rainfall intensity (t_2 in Fig. 7), the dilution effect was getting weaker. Soil CO_2 declined while most of it dissolved in the water and infiltrated into the spring in a short time, which caused a higher pCO_2, lower pH and stronger erosion. In this case, EC increased due to the dominance of soil CO_2 effect over the dilution effect (Liu et al., 2007).

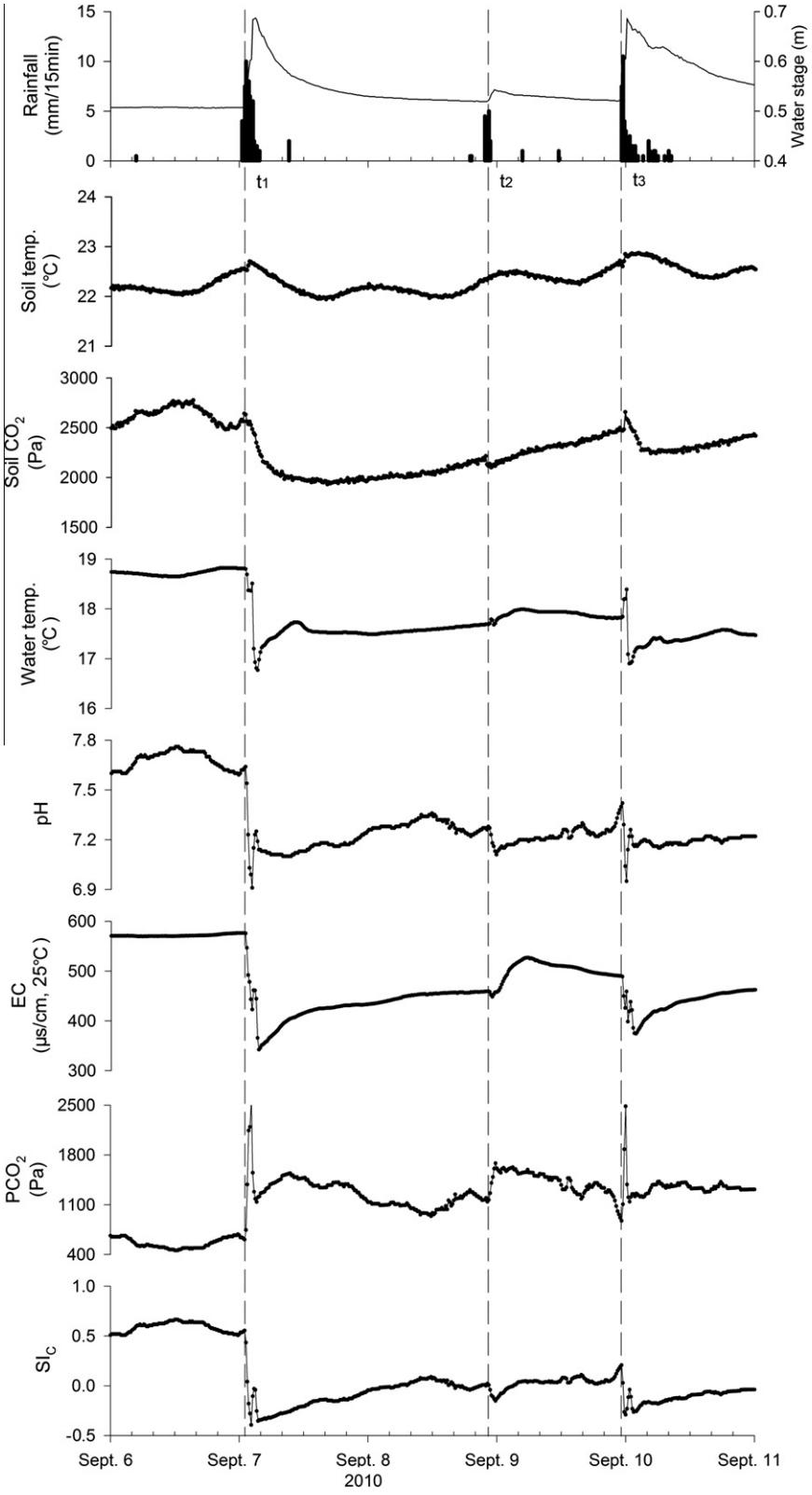

Fig. 7. Storm-scale variations in soil temperature, soil CO_2 concentrations on the sample soil plot and hydrochemical parameters in Wantian Spring at 15-min intervals, 6–11 September, 2010.

4.2.3. Calcite saturation

The variation of calcite saturation mirrors the pH variability which is regulated by the partial pressure of CO_2 in the water (Neal et al., 2002). As we have mentioned above, soil CO_2 variations caused the fluctuation of pCO_2 and thus affected the calcite saturation. Therefore, when soil CO_2 concentration was higher during spring-summer and the daytime (with a few hours time lag), there were higher pCO_2, lower pH and calcite saturation, and vice versa (Figs. 5, 6a and b). In the dry season, calcite saturation index was always above zero (Fig. 5), implying that the water was oversatu-

rated with respect to calcite and there existed release of CO_2 from water in the epikarst system. However, calcite saturation generally decreased below zero after rainfall and showed inverse variation with water stage (Figs. 5 and 7). This is mainly due to the rapid dissolution and infiltration of the soil CO_2.

4.3. Implications for the karst processes-related carbon cycle study

The karst processes-related carbon cycle, as a result of the water–carbonate rock–CO_2 gas–aquatic organism interaction, is a complex process. Soil CO_2, which is generated by root respiration and microbial decomposition, plays an important role in karst system as the driving forces for the karst processes. The factors controlling these processes could be climate (mainly rainfall and temperature), vegetation and soil (land use and land cover change – LUCC). Changes in temperature, rainfall and LUCC could thus regulate the generation, migration and conversion of soil CO_2. These variations finally determine the hydrochemical changes in the karst groundwater. However, it is difficult to distinguish them because of their combined and/or counterbalancing actions (e.g. dilution effect versus soil CO_2 effect) in nature. Therefore, further studies need be combined with some simulative and/or modeling experiments under controlled conditions.

In addition, this study has shown the high sensitivity and variability of epikarst processes to environmental change, implying that the role of karst processes in the global carbon cycle needs to be reappraised based on high-resolution monitoring strategy.

5. Conclusions

We have examined the direct correlation between the hydrochemical parameters in epikarst systems and soil CO_2 under different weather conditions. An epikarst spring system at Chenqi, Puding, SW China was chosen to monitor both the concentration of soil CO_2 and hydrochemical parameters at high-resolution (every 15 min) during July 2010–December 2011 covering a complete hydrologic year, and to investigate the response of hydrochemical changes to soil CO_2 and weather conditions. It was found that both soil CO_2 and rainfall are the major driving forces for the hydrochemical variations in the epikarst system. The soil CO_2 effect on hydrochemical variations was reflected in all seasonal, diurnal and storm-scales. That is higher pCO_2, lower pH and higher EC caused by higher soil CO_2 in spring-summer, while lower pCO_2, higher pH and lower EC caused by lower soil CO_2 in autumn–winter. Similar variations were also found on diurnal scales but with a time lag of a few hours between hydrochemical changes and soil CO_2 change during dry season, showing effect of the groundwater recharge mode as well as the complexity of the supply path (quick flow by conduit or slow flow by fracture). During rainy seasons, hydrochemical changes in epikarst groundwater were regulated by both dilution and soil CO_2 effects. Under high-intensity rainfall, the dilution effect was dominant, indicated by the decrease in EC, pH and calcite saturation, but the increase in pCO_2. In contrast, during low-intensity rainfall, the CO_2 effect was dominant, indicated by the increase in EC and pCO_2 but the decrease in pH and calcite saturation.

To sum up, this study has shown the high sensitivity and variability of epikarst processes to eco-environmental change, implying that the role of karst processes in the global carbon cycle needs to be reappraised based on high-resolution monitoring strategy.

Acknowledgments

This work was supported by the Strategic Priority Research Program (XDA05070400) of the Chinese Academy of Sciences, the Hundred Talent Program (2006-067) and the National Natural Science Foundation of China (41172232,41103084). Special thanks are given to the two anonymous reviewers for their thoughtful comments and suggestions, which greatly improved the original draft.

References

Atkin, O.K., Edwards, E.J., Loveys, B.R., 2000. Response of root respiration to changes in temperature and its relevance to global warming. New Phytol. 147 (1), 141–154.

Atkinson, T., 1977. Diffuse flow and conduit flow in limestone terrain in the Mendip Hills, Somerset (Great Britain). J. Hydrol. 35 (1–2), 93–110.

Banks, D., Frengstad, B., 2006. Evolution of groundwater chemical composition by plagioclase hydrolysis in Norwegian anorthosites. Geochim. Cosmochim. Acta 70 (6), 1337–1355.

Beltrami, H., Kellman, L., 2003. An examination of short-and long-term air–ground temperature coupling. Global Planet. Change 38 (3), 291–303.

Birk, S., Liedl, R., Sauter, M., 2004. Identification of localised recharge and conduit flow by combined analysis of hydraulic and physico-chemical spring responses (Urenbrunnen, SW-Germany). J. Hydrol. 286 (1), 179–193.

Brook, G.A., Folkoff, M.E., Box, E.O., 1983. A world model of soil carbon dioxide. Earth Surf. Proc. Land. 8 (1), 79–88.

Cellier, P., Richard, G., Robin, P., 1996. Partition of sensible heat fluxes into bare soil and the atmosphere. Agric. For. Meteorol. 82 (1–4), 245–265.

Denić-Jukić, V., Jukić, D., 2003. Composite transfer functions for karst aquifers. J. Hydrol. 274 (1), 80–94.

Ford, D.C, Willams, P.W., 2007. Karst Hydrogeology and Geomorphology, second ed. Wiley, 562pp.

Hanson, P., Edwards, N., Garten, C., Andrews, J., 2000. Separating root and soil microbial contributions to soil respiration: a review of methods and observations. Biogeochemistry 48 (1), 115–146.

Jassal, R.S., Black, T.A., Drewitt, G.B., Novak, M.D., Gaumont-Guay, D., Nesic, Z., 2004. A model of the production and transport of CO_2 in soil: predicting soil CO_2 concentrations and CO_2 efflux from a forest floor. Agric. For. Meteorol. 124 (3–4), 219–236.

Jenkinson, D., Adams, D., Wild, A., 1991. Model estimates of CO_2 emissions from soil in response to global warming. Nature 351 (6324), 304–306.

Krawczyk, W.E., Ford, D.C., 2006. Correlating specific conductivity with total hardness in limestone and dolomite karst waters. Earth Surf. Proc. Land. 31, 221–234.

Lasco, R.D., Lales, J.S., Arnuevo, M., 2002. Carbon dioxide (CO_2) storage and sequestration of land cover in the Leyte Geothermal Reservation. Renew. Energy 25 (2), 307–315.

Liu, Z., Groves, C., Yuan, D., Meiman, J., Jiang, G., He, S., Li, Q., 2004. Hydrochemical variations during flood pulses in the south-west China peak cluster karst: impacts of $CaCO_3$–H_2O–CO_2 interactions. Hydrol. Process. 18 (13), 2423–2437.

Liu, Z., Li, Q., Sun, H., Liao, C., Li, H., Wang, J., Wu, K., 2006. Diurnal variations of hydrochemistry in a travertine-depositing stream at Baishuitai, Yunnan, SW China. Aquat. Geochem. 12 (2), 103–121.

Liu, Z., Li, Q., Sun, H., Wang, J., 2007. Seasonal, diurnal and storm-scale hydrochemical variations of typical epikarst springs in subtropical karst areas of SW China: soil CO_2 and dilution effects. J. Hydrol. 337 (1–2), 207–223.

Liu, Z., Dreybrodt, W., Wang, H., 2010. A new direction in effective accounting for the atmospheric CO_2 budget: considering the combined action of carbonate dissolution, the global water cycle and photosynthetic uptake of DIC by aquatic organisms. Earth Sci. Rev. 99 (3–4), 162–172.

Liu, Z., Dreybrodt, W., Liu, H., 2011. Atmospheric CO_2 sink: silicate weathering or carbonate weathering? Appl. Geochem. 26, S292–S294.

Manabe, S., Stouffer, R.J., 1979. A CO_2-climate sensitivity study with a mathematical model of the global climate. Nature 282, 491–493.

Morse, J.W., Arvidson, R.S., 2002. The dissolution kinetics of major sedimentary carbonate minerals. Earth Sci. Rev. 58 (1–2), 51–84.

Neal, C., Watts, C., Williams, R.J., Neal, M., Hill, L., Wickham, H., 2002. Diurnal and longer term patterns in carbon dioxide and calcite saturation for the River Kennet, south-eastern England. Sci. Total Environ. 282, 205–231.

Raich, J.W., Schlesinger, W.H., 1992. The global carbon dioxide flux in soil respiration and its relationship to vegetation and climate. Tellus B 44 (2), 81–99.

Sun, H.G., Han, J.T., Zhang, S.R., Lu, X.X., 2011. Transformation of dissolved inorganic carbon (DIC) into particulate organic carbon (POC) in the lower Xijiang River, SE China: an isotopic approach. Biogeosci. Discuss. 8, 9471–9501.

Wigley, T., 1977. WATSPEC: a computer program for determining the equilibrium speciation of aqueous solutions. Brit. Geomorphol. Res. Group Tech., Bull. 20, 1–48.

Yuan, D., 1997. The carbon cycle in karst. Z. Geomorphol. 108, 91–102.

Zhao, M., Zeng, C., Liu, Z., Wang, S., 2010. Effect of different land use/land cover on karst hydrogeochemistry: a paired catchment study of Chenqi and Dengzhanhe, Puding, Guizhou, SW China. J. Hydrol. 388 (1–2), 121–130.

Zolotov, A.Y., Ivanov, V., Amelin, V., 2002. Methods and Tools for Analysis of Liquid Samples. Comprehensive Analytical Chemistry. Elsevier, pp. 69–117 (Chapter 3).